Topological Research and Comparison of Low Harmonic Input Three-Phase Rectifier with Passive Auxiliary Circuit

Zhong Chen, Yingpeng Luo and Yinyu Zhu
Aero-Power Sci-tech Center
Nanjing University of Aeronautics & Astronautics
Nanjing, P.R. China
Email: chenz@nuaa.edu.cn

Abstract—**A novel passive correction approach is proposed in this paper. By adding a passive auxiliary circuit to the ac side of the rectifier with dc-side C filter, the input currents and power factor can be improved. According to distinctive configurations of the auxiliary circuits, eight low harmonic input rectifier topologies are derived. Three rectifier topologies with better comprehensive performance are deeply analyzed and compared in operation principle, auxiliary circuit design and characteristic discussion. Experimental results from the prototypes are shown to confirm the validity of the analysis and the feasibility of the proposed approach.**

I. INTRODUCTION

Conventional three-phase rectifiers with dc-side C filter are widely used as the interface circuits between the grid and power electronic equipments for their simplicity and reliability. Because of the nonlinear characteristic of diodes, large mount of harmonics are drawn from the grid, leading to the severely distorted input currents and low power factor [1].

Reducing input current harmonics by modifying the rectifier itself mainly includes the following techniques: PWM rectifiers could improve the input currents effectively, but the shortcoming of large switching loss and unsatisfied efficiency limit its application especially in the high power application [2], [3]; Multiple pulse rectifiers could achieve acceptable input currents in relatively low cost and good EMI, but satisfied input current usually accompanies increase of pulse number, leading to heavier weight of the equipment [4], [5]; Rectifiers applying current injection contribute to the reduction of input current by injecting third order current harmonics into the input terminal of rectifier, but the method does not get widely used [6], [7]. Some novel rectifiers, such as RNSIC (rectifier with near-sinusoidal input currents) are proposed in recent years [8]-[9]. RNSIC rectifiers have caught increasing attention for their simple fabrication and high reliability, but research on them is inadequate and unsystematic.

Based on the former research, a novel passive correction approach is proposed in the paper. By adding an inductor capacitor auxiliary circuit to the input terminal of diode bridge rectifier, a family of low harmonic input three-phase rectifier is derived. They are only composed of passive components, preferable to work in high power application with high EMI requirement. Some important conclusions are drawn from the comparative analytical results of three typical rectifiers in operation principle and characteristic discussion. Experimental results from seven prototypes built in the laboratory are shown to confirm the validity of the analysis and the feasibility of the proposed correction approach.

II. TOPOLOGY OF LOW HARMONIC INPUT THREE-PHASE RECTIFIER WITH AUXILIARY CIRCUIT

A. Proposal of Novel Passive Correction Approach

By adding a passive auxiliary circuit to the input terminal of conventional uncontrolled rectifier (as Fig. 1(a) shown), a novel low harmonic input three-phase rectifier (as Fig. 1(b) shown) is obtained.

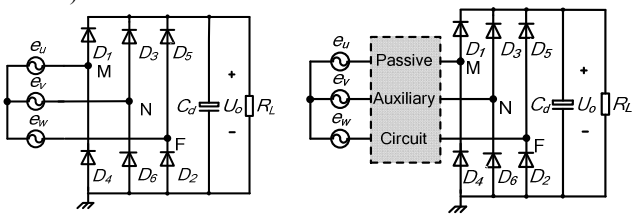

(a) conventional uncontrollable three-phase rectifier

(b) proposed rectifier with passive auxiliary circuit

Figure 1. Three-phase rectifier with dc-side C filter.

There are four basic configurations of the inductor and capacitor auxiliary circuit (as Fig. 2 shown). Auxiliary circuit

This work was supported by Doctoral Fund of Ministry of Education of China under Award 200802871033 and Aeronautical Science Foundation of China under Award 2009ZC52030.

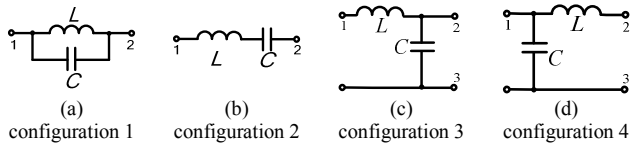

Figure 2. Four Basic configurations of *LC* auxiliary circuit.

1 [10-11] and 2 [12] are two-terminal network, while auxiliary circuit 3 and 4 are three-terminal network.

Fig. 3 illustrates eight topologies of low harmonic input three-phase rectifier with passive auxiliary circuit. By series connecting auxiliary circuit 1 and 2 to the ac-side of diode rectifier, topologies 1 and 2 will be arisen (as Fig. 3(a) and (b) shown); by connecting auxiliary circuit 3 and 4 to the ac-side of conventional rectifier, topologies 3 and 4 will be arisen(as Fig. 3(c) and (d) shown); by connecting terminal 1 and 2 of auxiliary circuit 3 and 4 to the ac-side of diode rectifier, terminal 3 to the dc bus of diode rectifier, topologies 5 [13] and 6 will be arisen(as Fig. 3(e) and (f) shown). Symmetrical versions of topologies 5 and 6 are named as topologies 7 and 8(as Fig. 3(g) and (h) shown).

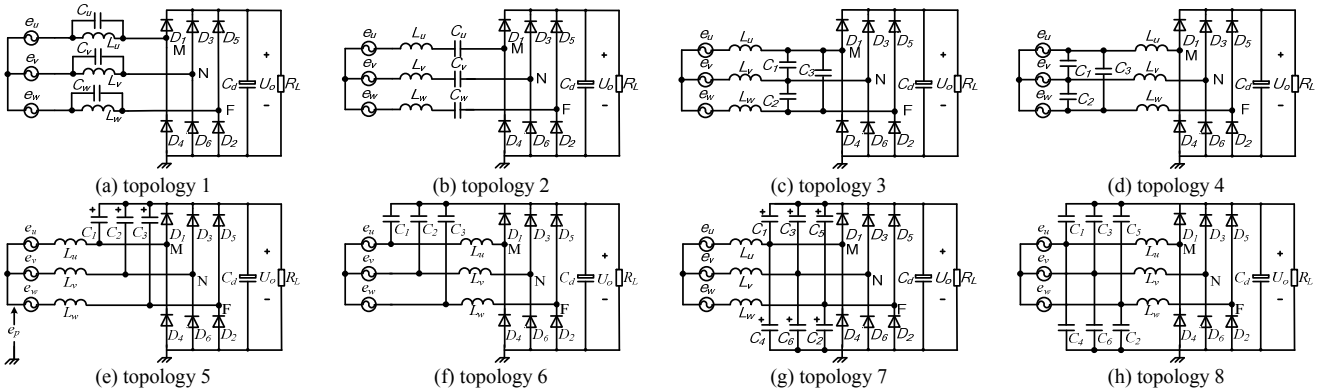

Figure 3. A family of low harmonic input three-phase rectifiers with passive auxiliary circuit.

Auxiliary circuit in topology 2 is another series passive filter, working as a band pass filter. This circuit is tuned at the fundamental frequency, exhibiting near zero impedance to the fundamental current but high impedance to the harmonic current. Following shortcomings limit its application: large value of passive components because of the small tuning frequency; unsatisfied harmonic suppression under load variation application because bandwidth of the filter is determined by the load. But it is a simple and effective unity power factor rectification in some special application [12].

In topology 4, 6 and 8, commutation capacitors of the auxiliary circuit which are parallel connected to the input terminal of rectifier contribute to high frequency harmonics filtering and reactive power compensation. But value of the capacitors is not easy to determine in practical application.

For topology 3, 5 and 7, former researches show that near sinusoidal input currents and high power factor will be achieved with optimal design of the auxiliary circuit [8-9, 13]. These three rectifier topologies catch more and more attention in the recent years.

In this paper, topology 3, 5 and 7 are picked up to be comparatively investigated and analyzed in operation principle, and characteristic discussion to reveal some general rules of this family of rectifiers. For convenient analysis, topology 3, 5 and 7 are named as RNSIC-2, RNSIC-3, and RNSIC-1.

B. Comparisons Between the Eight Topologies

Auxiliary circuit in topology 1 which is actually a series passive filter can be considered as the dual form of parallel tuning filter [14]. The series passive filter consists of parallel-resonant LC circuit, each tuned at a harmonic frequency, thus acting as a harmonic current dam. On the other hand, if satisfied harmonics suppression performance is desired, several series passive filters with different tuning frequency must be set, thus increasing the number and weight of the passive components and limiting the usage of this topology.

III. OPERATION PRINCIPLE

As Fig. 3 shows, RNSIC converters are composed of three series inductors L_u, L_v, L_w of equal inductance values L and commutation capacitors of equal capacitance values C. Commutation capacitors are C_1-C_6 in RNSIC-1 but C_1-C_3 in RNSIC-2 and RNSIC-3.

For the sake of simplicity, following simplifications are perfumed: The mains currents are purely sinusoidal, no phase displacement between voltages and current.

$$e_u = U_M \sin \omega t, \quad i_u = I_M \sin \omega t \tag{1}$$

$$e_v = U_M \sin(\omega t - \frac{2}{3}\pi), \quad i_v = I_M \sin(\omega t - \frac{2}{3}\pi) \tag{2}$$

$$e_w = U_M \sin(\omega t + \frac{2}{3}\pi), \quad i_w = I_M \sin(\omega t + \frac{2}{3}\pi) \tag{3}$$

Where U_m is the amplitude of phase voltage, I_m is the amplitude of input currents.

Zero time point (t=0) is defined as the moment when the current i_u crosses zero from negative to positive, and t_1 is defined as the moment when the capacitor C_1 finishes discharging. As t_1 decreases, operation mode of RNSIC converters changes from small current mode to medium current mode and large current mode. In RNSIC converters, commutation capacitors start charging or discharging when the currents through diodes cross zero. In RNSIC-1 and RNSIC-3, when diodes conduct, currents through them are the input

TABLE I. START TIME, END TIME AND DURATION OF THE CURRENT DISCHARGING C_1

Converter	Operation Mode	Start time	End time (ωt_1)	Duration
RNSIC-1 RNSIC-3	Large Current	0	(0,π/3)	(0,π/3)
	Medium Current		(π/3,2π/3)	(π/3,2π/3)
	Small Current		(2π/3,π)	(2π/3,π)
RNSIC-2	Large Current	0	(0,π/3)	(0,π/3)
	Medium Current	(0, π/6)	(π/3,π/2)	π/3
	Small Current	π/6	(π/2,5π/6)	(π/3,2π/3)

currents, so capacitors start charging or discharging when the input currents cross zero; while in RNSIC-2, when diodes conducts, currents through them comprise the sum of input currents and the currents through commutation capacitors. Start time, end time and duration of the currents discharging commutation capacitors vary with the load, as Table I shown.

A. Large Current Mode

When RNSIC converters work in the large current mode, t_1 varies in the interval [0, π/(3ω)]. As Fig. 4 illustrates, in large current mode, diodes of RNSIC converters conduct in the same sequence. Two distinct operation stages in which two or three diodes conduct exist and conduction time of the diodes is π/ω-t_1. As Fig. 5 illustrates, in RNSIC-1 and RNSIC-2, the dc side current i_o has the same waveform, a twelve-pulse waveform with different width; while in RNSIC-3, i_o is a six-pulse waveform with different width.

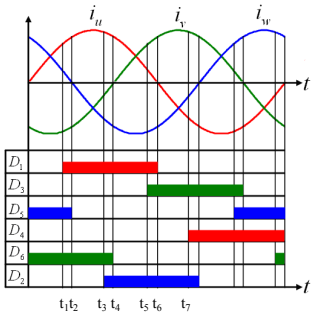

Figure 4. Key waveforms of RNSIC converters in large current mode.

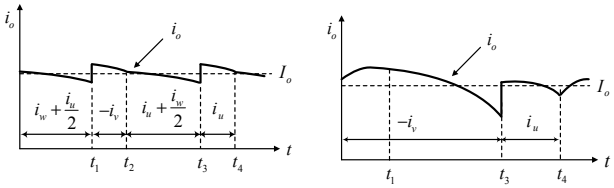

(a) RNSIC-1 and RNSIC-2 (b) RNSIC-3

Figure 5. I_o of RNSIC converters in large current mode.

I_o, the mean value of i_o in RNSIC-1 and RNSIC-2 could be expressed as follow:

$$I_o = \frac{3}{\pi}\left[\int_0^{\omega t_1}\left(I_m \sin(\omega t + \frac{2}{3}\pi) + \frac{1}{2} I_m \sin \omega t\right) d\omega t + \int_{\omega t_1}^{\frac{\pi}{3}} -\frac{1}{2} I_m \sin(\omega t - \frac{2}{3}\pi) d\omega t\right] \quad (4)$$

In RNSIC-3, I_o could be expressed as follow:

$$I_o = \frac{3}{2\pi}\left[\int_0^{\frac{\pi}{3}+\omega t_1} -I_m \sin(\omega t - \frac{2\pi}{3}) d\omega t + \int_{\frac{\pi}{3}+\omega t_1}^{\frac{2\pi}{3}} I_m \sin \omega t d\omega t\right] \quad (5)$$

By simplifying (4) and (5), I_o in three RNSIC converters will be expressed as follow:

$$I_o = \frac{3}{2\pi} I_m (1 + \cos \omega t_1) \quad (6)$$

B. Medium Current Mode

When RNSIC converters work in medium current mode, t_1 varies in the interval [π/(3ω), 2π/(3ω)] for RNSIC-1 and RNSIC-3, but in the interval [π/(3ω), π/(2ω)] for RNSIC-2.

As Fig. 6 illustrates, in RNSIC-1 and RNSIC-3, diodes conduct in the same sequence, two distinct operation stages in which one or two diodes conduct exist; while in RNSIC-2, two diodes conducts at any time, conduction time of the diodes and capacitors discharging duration fix to be 2π/(3ω) and π/(3ω).

As Fig. 7 illustrates, i_o has distinctive waveform in RNSIC converters. In RNSIC-1, i_o is a twelve-pulse waveform with different width; in RNSIC-2, i_o is six-pulse waveform with same width; in RNSIC-3, i_o gets discontinuous. In RNSIC-3, when the only conducting diode is the upper diode, i_o becomes discontinuous for no path exists for the input currents flowing. Expressions of I_o in this mode are given in Table II.

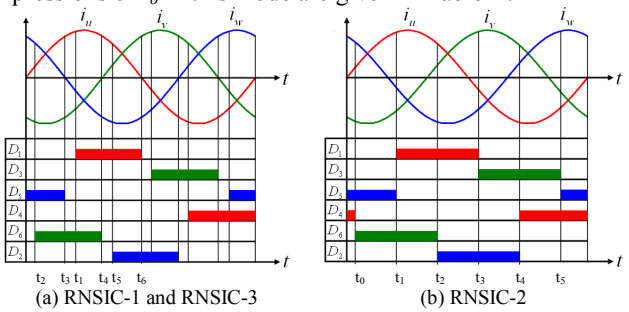

(a) RNSIC-1 and RNSIC-3 (b) RNSIC-2

Figure 6. Key waveforms of RNSIC converters in medium current mode.

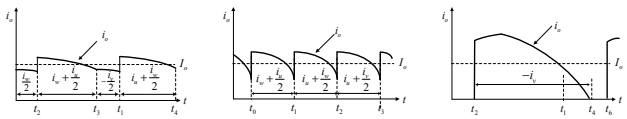

(a) RNSIC-1 (b) RNSIC-2 (c) RNSIC-3

Figure 7. I_o of RNSIC converters in medium current mode.

C. Small Current Mode

When RNSIC converters work in the small current mode, t_1 varies in the interval [2π/(3ω), π/ω] for RNSIC-1 and RNSIC-3, but in the interval [π/(2ω), 5π/(6ω)] for RNSIC-2. As Fig. 8 illustrates, in RNSIC-1 and RNSIC-3, diodes conduct in the same sequence, two distinct operation stages in

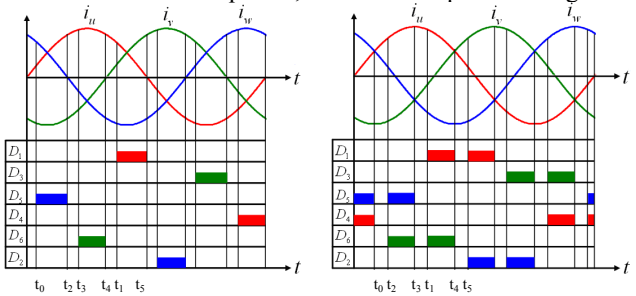

(a) RNSIC-1 and RNSIC-3 (b) RNSIC-2

Figure 8. Key waveforms of RNSIC converters in small current mode.

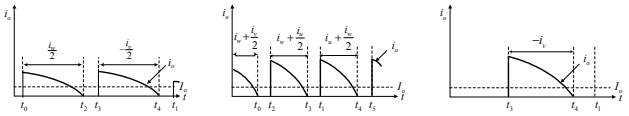

(a) RNSIC-1 (b) RNSIC-2 (c) RNSIC-3

Figure 9. I_o of RNSIC converters in small current mode.

TABLE II. EXPRESSIONS OF I_O IN RNSIC CONVERTERS

Converter	Operation Mode	Expressions of I_o
RNSIC-1 RNSIC-3	Large Current	$I_o = \frac{3}{2\pi} I_m (1+\cos\omega t_1)$
	Medium Current	
	Small Current	
RNSIC-2	Large Current	
	Medium Current	$I_o = \frac{3\sqrt{3}}{2\pi} I_m \cos(\omega t_1 - \frac{\pi}{6})$
	Small Current	$I_o = \frac{3\sqrt{3}}{2\pi} I_m (1+\cos(\omega t_1 + \frac{\pi}{6}))$

which none or one diode conducts exist, and conduction time of the diodes is π/ω-t_1. While in RNSIC-2, two distinct operation stages in which none or two diodes conducts exist, and conduction time of the diodes is $5\pi/(3\omega)$-$2t_1$.

As Fig. 9 illustrates, i_o becomes discontinuous in RNSIC converters. In RNSIC-1 and RNSIC-2, i_o is a six-pulse waveform; while in RNSIC-3, i_o is three-pulse waveform. Expressions of I_o in this mode are given in Table II.

From above analysis, following conclusions are drawn:

1) For RNSIC converters, three operation modes exist. When working in large current mode, RNSIC-1 and RNSIC-2 have same equivalent circuit, input characteristic and output characteristic. In RNSIC-1 and RNSIC-3, diodes conduct in the same sequence, mean value of the dc side current i_o has the same expression, but different waveforms does i_o have.

2) In RNSIC converters, dc side current i_o would become discontinuous in at least one operation mode. But the reason why i_o become discontinuous is different in RNSIC-2 and RNSIC-3. In RNSIC-2, commutation capacitors are located in ac side of the rectifier, so the grid provides power to the load when at least two diodes conduct. In RNSIC-3, commutation capacitors are only parallel connected to the upper diode, so i_o become discontinuous when no lower diode conducts.

IV. CHARACTERISTIC DISCUSSION

A. Optimal Value of Auxiliary Circuit

Fig.10 presents the variation of the optimal capacitance C as a function of the input voltage U_m in RNSIC converters.

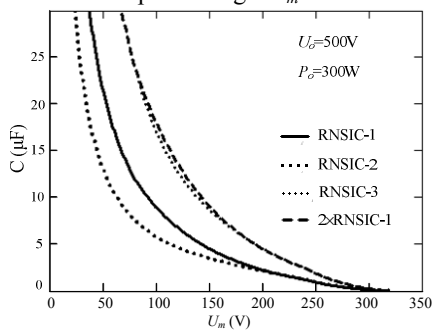

Figure 10. Variations of C as a function of U_m in RNSIC converters.

The values of P_o and U_o are adopted as 300 W and 500V. Optimal capacitances of auxiliary circuit have similar characteristic in three RNSIC converters. As the input voltage increases from low to high, optimal value of capacitance will decrease. Optimal capacitance is the smallest in RNSIC-2 but largest in RNSIC-3. Optimal capacitance of RNSIC-3 is nearly twice time as large as that of RNSIC-1. Moreover, as the output power increases, optimal capacitance will increase.

Fig.11 presents the variation of the optimal inductance L as a function of the input voltage U_m and the output power P_{out} in RNSIC converters. The values of U_o are adopted as 500 V, and the values of P_o are adopted as 300W and 1000 W, respectively. As U_m increases from low to high, optimal value of inductance will increase. But after RNSIC rectifiers enter into large current mode, the optimal inductance will decrease. As P_o is increased, the optimal inductance will decrease.

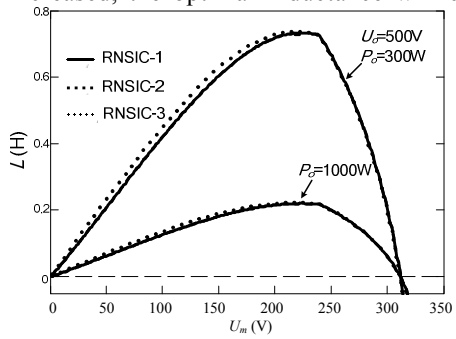

Figure 11. Variations of L as a function of U_m in RNSIC converters.

B. External Characteristic

Dc side current ripple is a key issue for the selection of electrolytic capacitor. Equation (7) and (8) give the expression of root mean square current ripper factor.

$$i_o = I_o + \sum_{n=1}^{\infty} I_n \sin(n\omega t + \varphi_n) \tag{7}$$

$$\frac{I_{AC}}{I_o} = \frac{\sqrt{i_o^2 - I_o^2}}{I_o} \tag{8}$$

Fig.12 shows the variation of dc side current ripple factor and normalized output voltage of RNSIC converters. As Fig. 12(a) illustrates, dc side current ripple of RNSIC converters has following properties: *1)* as ωt_1 increases, dc side current ripple will be increased; *2)* dc side current ripple is smallest in RNSIC-1 under same I_o. As Fig. 12(b) illustrates, output voltage of RNSIC converters have similar properties: As load resistor is increased, output voltage will increase.

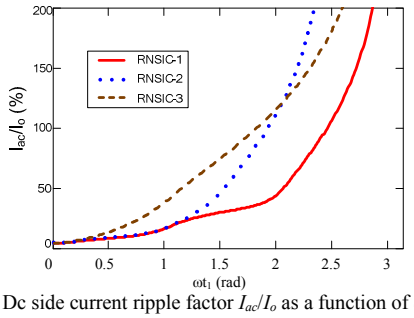

(a) Dc side current ripple factor I_{ac}/I_o as a function of ωt_1

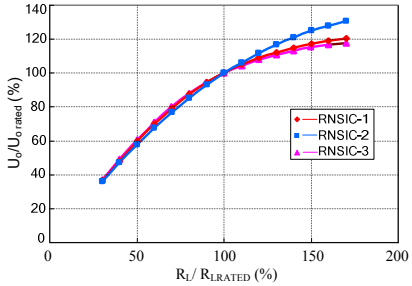

(b) Normalized output voltage U_o as a function of normalized load resistor

Figure 12. Output characteristics of RNSIC converters.

Fig.13 presents the variation of input current THD and power factor of RNSIC converters as a function of normalized load resistor. Input current THD is slightly influenced by the load resistor, all below 2%; input power factor is strongly influenced by load resistor. When the load resistor deviates from the rated value, power factor decreases drastically.

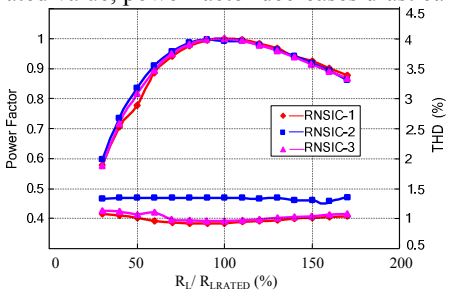

Figure 13. Input characteristics of RNSIC converters.

V. EXPERIMENTAL RESULTS

In order to verify the feasibility of the analysis derived above, seven RNSIC prototypes are built and tested in laboratory. Detail specifications are given in Table III. Topologies of prototype 1-5 are RNSIC-1, while topologies of prototype 6 and 7 are RNSIC-2 and RNSIC-3, respectively. Prototype 1, 4, 6 and 7 all work in large current mode, with the same design value of ωt_1 corresponding to 0.307π; Prototype 2 and 3 work in medium current mode and small current mode, with the design value of ωt_1 corresponding to 0.518π and 0.741π, respectively.

TABLE III. SPECIFICATION OF SEVEN RNSIC PROTOTYPES

Prototype	U_m /V	U_o / V	P_o / kW	L / mH	C / μF
1	250	500	7.18	27.7	22.46
2	150	500	6.55	27.7	98.7
3	55	500	2.52	27.7	159.2
4	250	500	4.79	41.5	14.92
5	250	515	7.95	27.7	27.7
6	250	500	7.18	27.7	22.46
7	250	500	7.18	27.7	44.88

Fig. 14 illustrates the experimental waveforms of i_u and e_u in seven prototypes. Input currents are nearly sinusoidal, and the displacement factors are all near unity. Input currents total harmonic distortion (THD) of prototype 1 is 4.656% (as Fig. 14.(h) shown), input currents THDs of other prototypes are all below 6% which are not given in Fig. 14. Additionally, power factors of seven prototypes are all higher than 0.99.

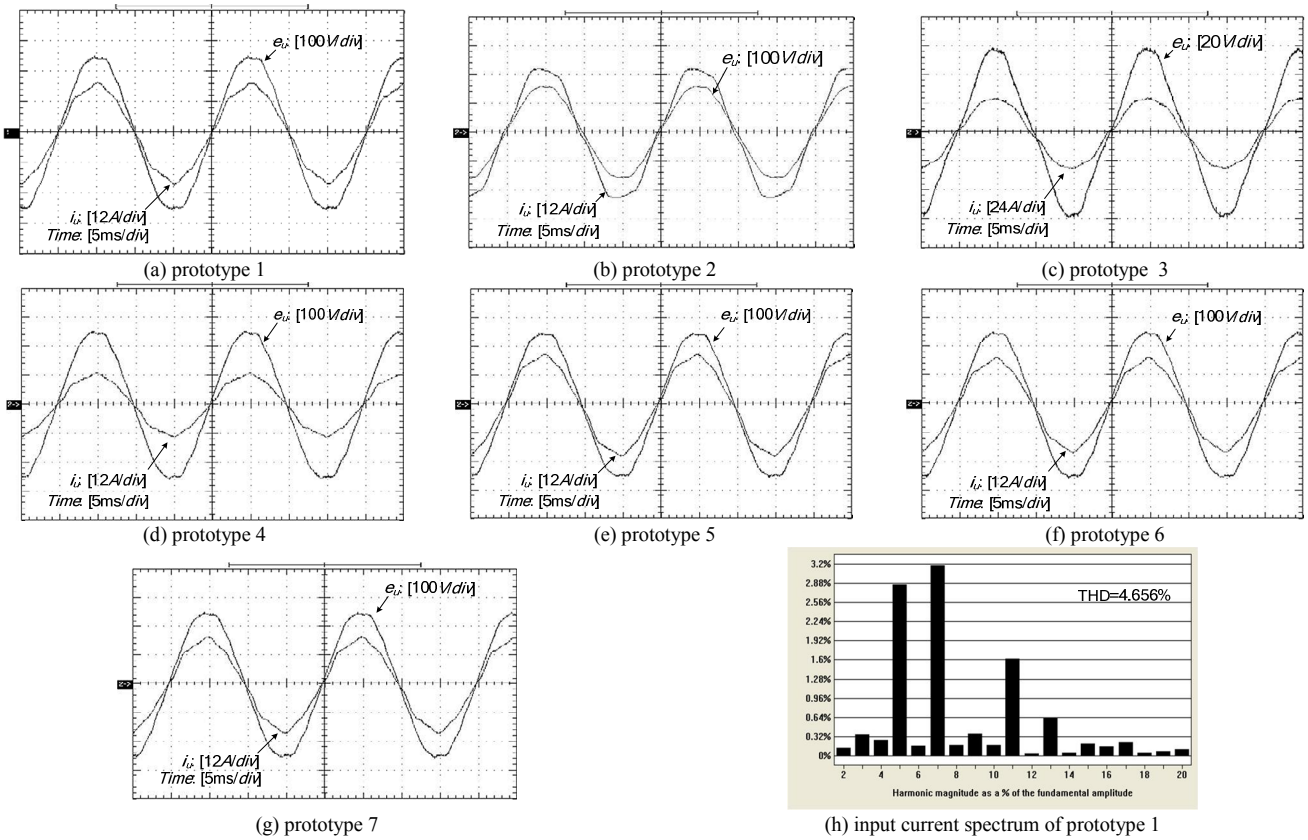

(a) prototype 1 (b) prototype 2 (c) prototype 3

(d) prototype 4 (e) prototype 5 (f) prototype 6

(g) prototype 7 (h) input current spectrum of prototype 1

Figure 14. Experimental waveforms of phase voltage and input current.

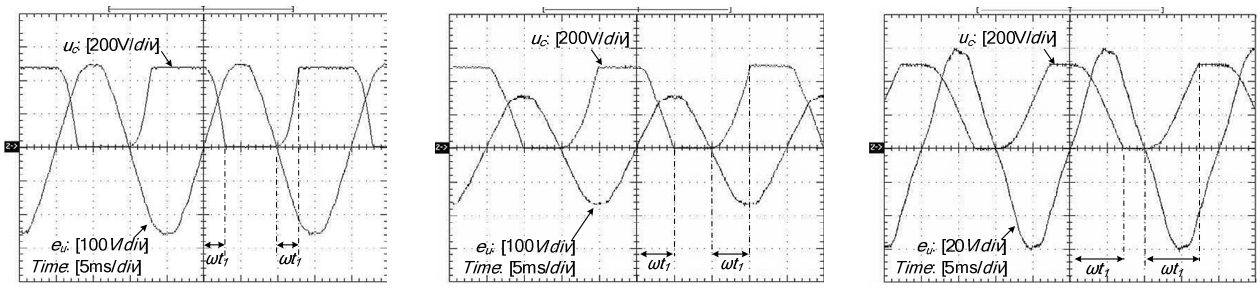

(a) prototype 1 (b) prototype 2 (c) prototype 3

Figure 15. Experimental waveforms of commutation capacitor voltage u_c.

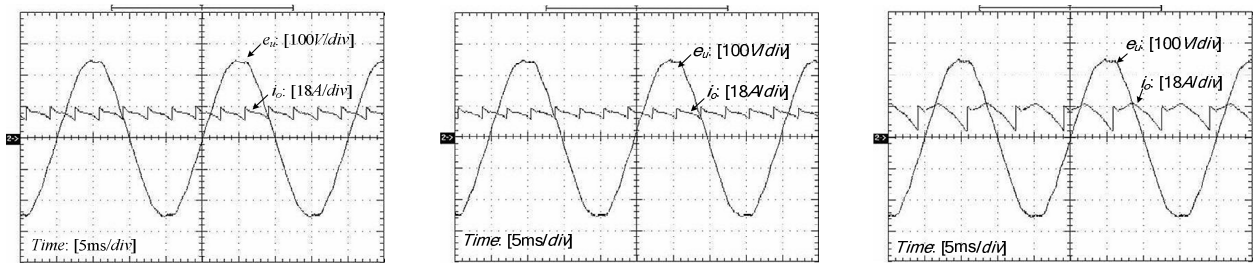

(a) prototype 1 (b) prototype 6 (c) prototype 7

Figure 16. Experimental waveforms of dc-side current i_o.

Fig. 15 illustrates the experimental waveform of u_c, commutation capacitors voltage in prototype 1, 2, and 3. Observed values of ωt_1 in the three prototypes are about 0.3π, 0.5π, and 0.7π, coinciding well with the design values.

Fig. 16 illustrates the experimental waveform of dc side current i_o in prototype 1, 6 and 7. When working under same application and in large current mode, i_o is the same 12-pulse waveform in RNSIC-1 and RNSIC-2, but 6-pulse waveform with large ripple in RNSIC-3, agreeing with above analysis.

VI. CONCLUSION

Based on four configurations of *LC* auxiliary circuit, a family of low harmonic input three-phase rectifiers with passive auxiliary circuit is proposed. Three topologies with better performance are selected to be deeply analyzed. Experimental results show that this family of rectifier with simple fabrication could effectively suppress the input current harmonics and improve power factor. Analytical results and character discussion in this paper provide reference for the analysis and application of other passive three-phase rectifier.

REFERENCES

[1] H. Akagi, E. H. Watanabe, and M. Aredes, *Instantaneous Power Theory and Applications to Power Conditioning*, New Jersey: John Willey & Sons, 2007, pp. 4-5.

[2] M. Malinowski, M.Jasinski, and M. P. Kazmierkowski "Simple Direct Power Control of Three-Phase PWM Rectifier Using Space-Vector Modulation (DPC-SVM)," *IEEE Trans. Ind. Electron.*, vol. 51, pp. 447–454, Apr. 2004.

[3] H. Mao, F.C. Lee, D. Borojevie, and S. Hiti, "Review of High-Performance Three-Phase Power-Factor Correction Circuits," *IEEE Trans. Ind. Electron.*, vol. 44, pp. 437–446, Aug. 1997.

[4] B. Singh, G. Bhuvaneswari, and V. Garg, "T-Connected Autotransformer -Based 24-Pulse AC-DC Converter for Variable Frequency Induction Motor Drives," *IEEE Trans. Energy Conv.,* vol. 21, pp. 663-672, Sep. 2006.

[5] F.J.M. de Seixas and I. Barbi, "A 12kW three-phase low THD rectifier with high frequency isolation and regulated dc output," *IEEE Trans. Power Electron.*, vol. 19, pp. 371-377, Mar. 2004.

[6] N. Vázquez, H. Rodriguez, C. Hernández, E. Rodriguez, and J. Arau, "Three-Phase Rectifier With Active Current Injection and High Efficiency," *IEEE Trans. Ind. Electron.*, vol. 56, pp. 110-119, Jan. 2009.

[7] P. Pejovic and Z. Janda, "An analysis of three-phase low harmonic rectifiers applying the third-harmonic current injection," *IEEE Trans. Power Electron.*, vol. 14, pp. 391-407, May 1999.

[8] D. Alexa, A. Sîrbu, and D. Dobrea, "Topologies of three- phase rectifiers with near sinusoidal input currents," *Proc. Inst. Electr. Eng.—Elect. Power Appl.*, vol. 151, no. 6, pp. 673–678, Nov. 2004.

[9] D. Alexa, A. Sîrbu, and A. Lazăr, "Three-Phase Rectifiers with Near Sinusoidal Input Current and Capacitors Connected on the AC side," *IEEE Trans. Ind. Electron.*, vol. 53, pp. 1612–1620, Oct. 2006.

[10] A. R. Prasad, P. D. Ziogas, and S. Manias, "A novel passive waveshaping method for single-phase diode rectifiers," *IEEE Trans. Ind. Electron.*, vol. 37, pp. 521–530, Dec. 1990.

[11] J. S. Lai, D. Hurst, and T. Key, "Switch-Mode Power Supply Power Factor Improvement Via Harmonic Elimination Methods," in *Proc. APEC'91*, 1991, pp. 415-422.

[12] V. Vorperian and R. B. Ridley, "A Simple Scheme for Unity Power-factor Rectification for High Frequency AC Buses," *IEEE Trans. Power Electron.*, vol. 5, pp. 70–87, Jan. 1990.

[13] Y. P. Luo, Z. Chen, and Y. Y. Zhu. "Three-phase rectifier with near-sinusoidal input currents and capacitors parallel connected with the upper diodes," in proc. *IEEE IPEMC 2009*, 2009, pp. 1697-1702.

[14] F. Z. Peng, "Harmonic sources and filtering approaches," *IEEE Ind. Appl. Mag.*, vol. 7, pp. 18–25, 2001.